Int. J. Multiphase Flow Vol. 13, No. 3, pp. 345–355, 1987
Printed in Great Britain.

0301-9322/87 $3.00 + 0.00

INVERTED ANNULAR FLOW BOILING

Y. LEE and K. H. KIM
Department of Mechanical Engineering, University of Ottawa, Ottawa, Ontario K1N 6N5, Canada

(*Received* 1 *October* 1985; *in revised form* 22 *December* 1986)

Abstract—The convective heat-transfer coefficients of inverted annular flow film boiling in the region immediately downstream of the rewetting front in the bottom flooding mode were calculated and were found to agree very well with the experimental values. Also, the results of the analysis reconfirmed that having more accurate heat-transfer coefficients in a confined space immediately downstream of the rewetting front substantially improves the accuracy of the estimate for rewetting velocities.

1. INTRODUCTION

A previous analytical and experimental study on bottom flooding (Kim & Lee 1982) has shown that, in a confined flow channel, the rewetting temperature plays a dominant role in the rewetting process and that the heat-transfer coefficient distribution downstream of the rewetting front (so-called "dry" region) has a greater influence on the final analysis than has been assumed by many in the literature.

The flow regimes downstream of the propagating rewetting front may be identified as inverted annular, dispersed and single vapor flow. A photograph of flow regimes in the vicinity of the rewetting front obtained from our visual study is presented in figure 1. It may be seen that the flow just downstream of the front, which is generally called the inverted annular flow boiling region, resembles a concentric annulus with the core of liquid moving axially in steam vapor.

For inverted annular flow boiling, several attempts have been made in the past to correlate it with pool film boiling correlations, i.e. the classical Bromley correlation. The Bromley (1950) correlation and subsequent similar formulations which included the effects of convection and subcooling of the liquid do not, however, account for the presence of two-phase flow nor its unsteady nature.

The present study attempts to calculate the convective heat-transfer coefficient of the inverted annular flow film boiling in the immediately downstream region of the rewetting front in the bottom flooding mode. The inverted annular flow region is defined here as the region downsteam of the rewetting front where the wall temperature is higher than the rewetting temperature of that particular condition, and the thermodynamic vapor quality is $<3\%$ (Groeneveld & Gardiner 1977).

2. ANALYSIS

In the analysis, the inverted annular flow is modeled as a concentric annulus with the core of liquid moving axially in steam vapor, as idealized in figure 2. The vapor flow in the annulus gap is taken as turbulent flow.

From the liquid mass flux and void fraction, the average liquid velocity can be calculated. The velocity profile in the vapor gap of the inverted annular flow is part of an assumed concentric annulus velocity profile. This assumed profile spans a region from the channel wall to some imaginary point within the liquid layer where the velocity would be zero, as illustrated in figure 2. The actual velocity profile is that part of the assumed profile between the liquid interface and the channel wall. The region next to the outer tube wall ($R_o < r < R_m$) is referred to here as the outer region and the region next to the vapor–liquid interface ($R_m < r < R_i^*$) as the inner region, where R is the radius and r is the radial distance. The subscripts o, i and m refer to the outer and inner boundaries and the maximum velocity point, respectively.

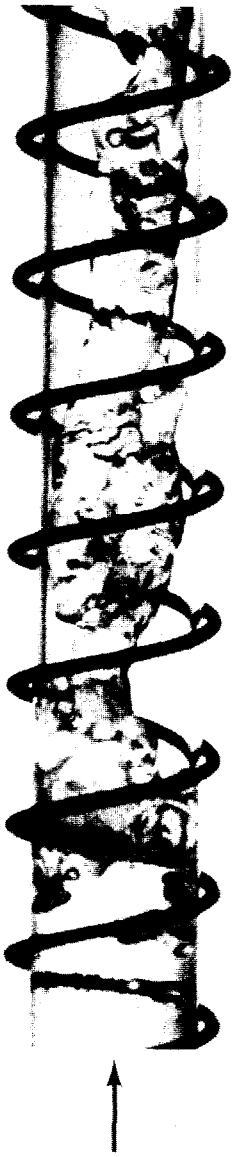

Figure 1. Flow visualization, inverted annular film region, $T_w \doteq 400^\circ C$.

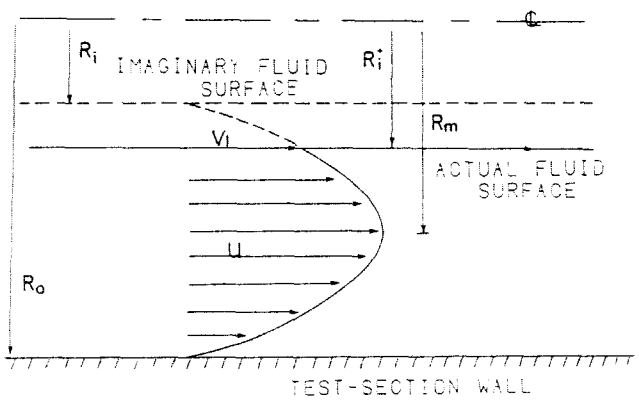

Figure 2. Idealized model, inverted annular film boiling.

2.1. *Vapor Velocity Profile and Reynolds Number*

Levy (1967), Roberts (1967) and Lee & Park (1971) are a few among many who have proposed different models for the velocity profile in a concentric annulus.

Lee & Park (1971) used Reichardt's (1951) expression for the eddy diffusivity of momentum together with a linear shear stress distribution for the derivation of a reasonably simple velocity profile in the developing flow. Their rationale was that as long as the choice of the shear stress distribution is consistent with one that agrees well with experimental results, a function of the shear stress distribution which would lead to a much simpler and more convenient velocity profile than those given by Levy (1967) would seem to be more practical. According to Deissler's (1955) study, the variation of the shear stress across the flow boundary layers has a negligible effect on the velocity distributions.

The modified Reichardt expression for the eddy diffusivity of momentum, ϵ_M, for a concentric annulus may be written as

$$\frac{\epsilon_M}{\nu} = \frac{K}{6}\left|(R - R_m)\right| \cdot \frac{u_{\tau R}}{\nu}\left[1 - \left(\frac{r - R_m}{R - R_m}\right)^2\right]\left[1 + 2\left(\frac{r - R_m}{R - R_m}\right)^2\right], \quad [1]$$

where ϵ_M is the eddy diffusivity for momentum, ν is the kinematic viscosity, K is the mixing-length constant, R_m is the radius of the maximum velocity and $u_{\tau R}$ is the shear velocity.

For the value of R_m, an empirical correlation of Leung *et al.* (1962), given here as [2], is used:

$$R_m = R_i\left[\frac{1 + (\alpha_1)^{1-n}}{1 + \left(\frac{1}{\alpha_1}\right)^n}\right], \quad [2]$$

where R_i and R_o are the radii of the inner core and outer tubes, respectively, $n = 0.343$ and $\alpha_1 = R_o/R_i$.

It is assumed that [1] is valid on both sides of the plane of zero shear and that the plane of zero shear is located at the maximum velocity point. For the outer region ($R_o < r < R_m$), the eddy diffusivity for momentum is obtained by having the mixing-length constant, K, the wall shear stress, τ_R and the radius, R as K_o, τ_{Ro} and R_o, respectively. Similarity, the diffusivity for the inner region ($R_m < r < R_i^*$) is derived by substituting K_i, τ_{Ri} and R_i into the equation.

Equating the eddy diffusivity at the plane of zero shear gives

$$\frac{K_o}{K_i} = \frac{R_m - R_i}{R_o - R_m}\left(\frac{\tau_{Ri}}{\tau_{Ro}}\right)^{0.5}. \quad [3]$$

Also from a force balance, we obtain

$$\frac{\tau_{Ri}}{\tau_{Ro}} = \frac{R_o}{R_i} \cdot \frac{R_m^2 - R_i^2}{R_o^2 - R_m^2}. \quad [4]$$

From the Reynolds equation with the concept of eddy diffusivity for momentum, ϵ_M, application of the momentum theorem, gives an expression for shear stress, τ_r as

$$\tau_r = \rho(\nu + \epsilon_M)\frac{du}{dy}, \quad [5]$$

where ρ is the fluid density, u is the velocity along the x-axis and y is the distance normal to the axis. Combining [1] and [5], and the linear shear stress distribution, together with non-dimensionalization and integration, we obtain

$$u_j^+ = -\frac{3}{\psi_j}\left|R_m^+ - R_j^+\right| \cdot \ln\left|\frac{K_j \cdot \delta_j^+ - 4K_j \cdot \delta_j^+ \cdot \eta_j^2 - \psi_j}{K_j \cdot \delta_j^+ - 4K_j \cdot \delta_j^+ \cdot \eta_j^2 + \psi_j}\right| + C_j, \quad [6]$$

where

$$\delta_j^+ = |R_m^+ - R_j^+|,$$

$$\eta_j = \frac{\delta_j^+ - y_j^+}{\delta_j^+},$$

$$\psi_j = (9K_j^2 \cdot \delta_j^{+2} + 48K_j \cdot \delta_j^+)^{\frac{1}{2}},$$

$$u_j^+ = \frac{u_j}{u_{\tau j}}, \quad y_j^+ = y_j \cdot \frac{u_{\tau j}}{\nu}$$

and

j = i or o, a dummy variable.

The constant C_j is obtained by forcing the velocity profile to pass through the point $u_j^+ = 12.8$, $y_j^+ = 26$. A value of 0.4 for K_o was used in the analysis as it has been shown (Levy 1967; Lee & Park 1971) that the mechanism of flow outside of the radius of maximum velocity in a concentric annulus is very similar to that which occurs in pipe flow.

For the regions very close to each wall (i.e. sublayers), we forced the core region velocity profile u^+ to pass through the point $y^+ = 26$, $u^+ = 12.8$, in accord with the experimental results of Lee & Park (1971). Therefore, the sublayer velocity profile also has to pass through the point. The modified Von Karman sublayer velocity profiles are

$$0 \leqslant y^+ \leqslant 5, \quad u^+ = y^+$$

$$5 \leqslant y^+ \leqslant 26, \quad u^+ = 4.73 \ln y^+ - 2.61. \qquad [7]$$

The Reynolds number of vapor, Re, in the annular gap may be expressed from the definition, in terms of the vapor mass flow rate, G_v, as

$$\mathrm{Re} = \frac{u_b 2(R_o - R_i^*)}{\nu} = \frac{2G_v}{\pi\mu_v(R_o + R_i^*)}, \qquad [8]$$

where u_b is the average vapor velocity, R_i^* is the radius of the liquid core, as illustrated in figure 2, and μ_v is the dynamic viscosity of the vapor.

The average vapor velocity, u_b, may be obtained from either the given vapor mass flow rate, G_v, or the vapor velocity profile.

The Reynolds number may also be obtained from the known velocity profile:

$$\mathrm{Re} = \frac{4}{b+1}\left[\frac{1}{R_i^{*+}}\int_{y_i^{*+}}^{y_{mi}^+} u_i^+(y_i^+ + R_i^+)\,dy_i^+ + \frac{b}{R_o^+}\int_0^{y_{mo}^+} u_o^+(R_o^+ - y_o^+)\,dy_o^+\right], \qquad [9]$$

where $b = R_o/R_i^*$, $y_i^* = R_i^* - R_i$, $y_{mi} = R_m - R_i$, $y_i = r - R_i$, $y_{mo} = R_o - R_m$, $y_o = R_o - r$ and the subscript m refers to the maximum velocity point.

With the above information, one may obtain by iteration the inner radius R_i and shear stresses, τ_j, as well as the vapor profile in the annulus gap.

2.2 Energy Equation and Heat-transfer Coefficient

The governing energy equation is obtained for the element in the fluid flow and, with a known heat flux ratio distribution, the heat flux at the channel wall is calculated.

If we let the heat flux distribution across the annular gap be $q/q_o = f(r)$, and the turbulent Prandtl number unity, the governing energy equation for the element may be given as:

(*a*) *for the outer region of the maximum velocity*,

$$\frac{\rho c_p(T_w - T_j)}{q_o} u_{\tau o} = \mathrm{Pr}\int_0^{y_j^+} \frac{f(r)\,dy^+}{1 + \mathrm{Pr}\,\dfrac{\epsilon_M}{\nu}} \qquad [10a]$$

where c_p is the specific heat, T is the temperature, q is the heat flux, Pr is the Prandtl number and the subscripts w, o and i refer to the wall, outer and inner, respectively;

(b) for the inner region of the maximum velocity,

$$\frac{\rho c_p (T_j - T_s)}{q_o} u_{\tau i} = \mathrm{Pr} \int_{y_i^+}^{y_j^+} \frac{f(r)\, dy^+}{1 + \mathrm{Pr}\, \frac{\epsilon_M}{\nu}} \qquad [10b]$$

where the subscript s refers to saturation.

The differential equation for the heat flux distribution across the annular gap, $f(r)$, may be obtained from an energy balance made on the annular elements. Integration of the equation between R_o and r, with the assumptions that the heating boundary condition is of constant heat flux and that u may be replaced by u_b, would result in the following expression:

$$\frac{q}{q_o} = \frac{1}{r} \frac{\left(R_o - R_i^* \cdot \frac{q_i}{q_o}\right)}{(R_o^2 - R_i^{*2})} (r^2 - R_o^2) + \frac{R_o}{r}. \qquad [11]$$

The assumption that $u = u_b$ is reasonable because it has been shown by Barrow (1960) that, for established flow, the choice of function for the velocity profile, to obtain the heat flux distribution across the annular space for the case of asymmetric heating, has a very minor effect on the final heat-transfer calculation.

Substituting [11] into [10a] and [10b], we obtain

$$\begin{aligned}
\frac{\rho_v c_{pv} (T_w - T_s)}{q_o} u_{\tau wo} = {} & \frac{\mathrm{Pr}(R_o^+ - R_i^{*+} A)}{(R_o^{+2} - R_i^{*+2})} \int_0^{y_{mo}^+} \frac{(R_o^+ - y^+)\, dy^+}{1 + \mathrm{Pr}\, \frac{\epsilon_M}{\nu}} \\
& + \frac{\mathrm{Pr}(R_i^{*+} A \cdot R_o^{+2} - R_i^{*+2} \cdot R_o^+)}{(R_o^{+2} - R_i^{*-2})} \int_0^{y_{mo}^+} \frac{dy^+}{\left(1 + \mathrm{Pr}\, \frac{\epsilon_M}{\nu}\right)(R_o^+ - y^+)} \\
& + \frac{u_{\tau wo}}{u_{\tau wi}} \frac{\mathrm{Pr}(R_o^{+} - R_i^{*} A)}{(R_o^{+2} - R_i^{*2})} \int_{y_i^+}^{y_{mi}^+} \frac{(R_i^+ + y^+)\, dy^+}{1 + \mathrm{Pr}\, \frac{\epsilon_M}{\nu}} \\
& + \frac{u_{\tau wo}}{u_{\tau wi}} \frac{\mathrm{Pr}(R_i^{*} \cdot A \cdot R_o^{+2} - R_i^{*2} \cdot R_o^{+})}{(R_o^{+2} - R_i^{*2})} \cdot \int_{y_i^+}^{y_{mi}^+} \frac{dy^+}{\left(1 + \mathrm{Pr}\, \frac{\epsilon_M}{\nu}\right)(R_i^+ + y^+)},
\end{aligned} \qquad [12]$$

where R_o^{+} is R_o non-dimensionalized using $u_{\tau wi}$, R_i^{*+} is R_i^* using $u_{\tau wo}$ for parameter conformity, A is the ratio q_i/q_o and the subscript v refers to vapor.

The heat-transfer coefficient, h, is defined as

$$h = \frac{q_o}{(T_w - T_s)}. \qquad [13]$$

The heat flux at $r = R_i^*$ is

$$q_i = -\rho_l c_{pl} (\epsilon_M + \alpha) \left.\frac{\partial T}{\partial r}\right|_{r = R_i^*} = h_l (T_s - T_{b,l}), \qquad [14]$$

where α is the thermal diffusivity and the subscripts l and b refer to liquid and bulk, respectively.

The increase in liquid bulk temperature is defined as

$$\rho u_l c_p \pi R_i^{*2} \frac{dT_{bl}}{dx} = \int_0^{R_i^*} \rho u c_p 2\pi r\, dr \frac{\partial T}{\partial x}. \qquad [15]$$

From the energy balance and [14] and [15], with an assumed parabolic temperature profile, integration between 0 and R_i^* would give the expression for h_l as

$$h_l = \frac{\rho_l c_{pl}}{1.17B + 1.83D}, \qquad [16]$$

where

$$B = R_i^* \int_0^{R_i^*} \frac{\cos\left(\frac{r}{R_i^*}\frac{\pi}{2}\right) - 1}{r(\epsilon_M + \alpha)} dr \quad \text{and} \quad D = \int_0^{R_i^*} \frac{\sin\left(\frac{r}{R_i^*}\frac{\pi}{2}\right) dr}{(\epsilon_M + \alpha)}.$$

2.3. Vapor Mass Flux

From the energy balance on the vapor control volume, we obtain

$$2R_o q_o - 2R_i^* q_i = R_o^2(h_g - h_f)\frac{d\dot{G}_v}{dx} + R_o^2 \cdot \dot{G}_v \frac{dh_g}{dx}, \quad [17]$$

where h_g and h_f are the enthalpies of vapor and liquid, respectively, and $\dot{G}_v$ is the vapor mass flux, i.e. $G_v/\pi R_o^2$.

In our previous study (Kim & Lee 1982), the vapor superheat in the inverted annular film boiling was neglected. However, in the present study, some vapor superheat in the annulus vapor gap was considered. We assume that 10%† of the total heat from the tube wall was used for the vapor superheat. Therefore,

$$\pi R_o^2 \cdot \dot{G}_v \frac{dh_g}{dx} = 0.1(2\pi R_o q_o). \quad [18]$$

Substituting [18] into [17], we may obtain the increase in vapor mass flux along the x-direction, $d\dot{G}_v/dx$.

2.4. Computation

Now, with the information from subsection 2.1 above, one may obtain by iteration the inner radius R_i and shear stresses, τ_j, as well as the vapor profile in the annulus gap. The steps are:

(i) Assume a value for R_i.
(ii) Obtain the value of τ_{Ri} (shear stress at R_i) which satisfies the boundary condition (at $r^+ = R_i^{*+}$, $u^+ = V_i^+$; liquid velocity). Once τ_{Ri} is obtained, τ_{Ro} may be calculated from the force balance given by [4].
(iii) Calculate the Reynolds number between R_i^* to R_o (using [9]) and check this Reynolds number against the Reynolds number given by [8]. If the two Reynolds numbers are not same, then iterate again with the new value of R_i until the two Reynolds numbers are the same. Once the value of R_i is known, the wall shear stress and the vapor velocity profile may be easily obtained.

The convective heat-transfer coefficient, h, in the inverted annular flow region was calculated for various conditions. Since q_i is known from [14] and [16], we can calculate q_o via iteration using [11] and [12], and h from the definition given by [13].

3. RESULTS AND DISCUSSION

In the present study, heat-transfer coefficients in the inverse annular flow region of a single tube in the bottom flooding mode were calculated.

Comparison of the analysis with experimental results as well as with the Bromley correlation showed that the present analysis on the heat transfer in the inverted annular flow region is a significant improvement over the Bromley or other pool boiling based correlations.

Figure 3 shows the effect of the initial wall temperature on the heat-transfer coefficients. Experimental convective heat-transfer coefficients were obtained from the experimental temperature–time trace curves (T–T plots) of Kim & Lee (1982). By knowing the slope of the temperature drop with time, the total heat-transfer rate at a given moment of time is calculated from an energy balance.

†The difference in calculated rewetting velocity using this assumption is about 3% compared to the case of no vapor superheat.

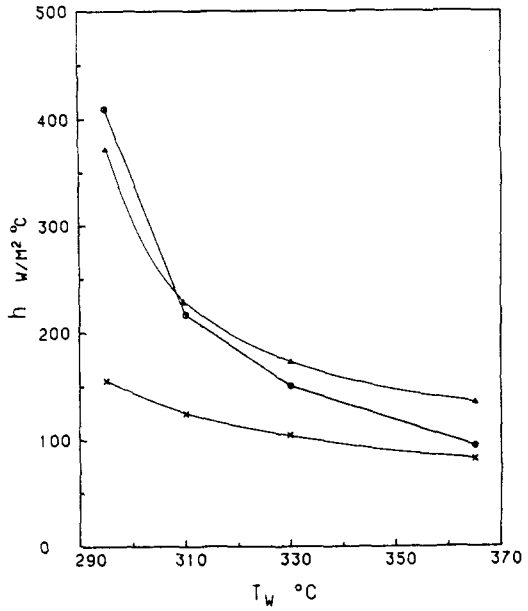

Figure 3. Effect of initial wall temperature. $G = 200\ \text{kg/m}^2\text{s}$, $T_c = 60°\text{C}$. ○, Experimental; ▲, present analysis; ×, Bromley-type equation.

The experimental heat-transfer coefficient is also compared with a Bromley-type heat-transfer coefficient (Clement *et al.* 1977). In our previous model (Kim & Lee 1982) for bottom flooding, a Bromley-type equation was used to calculate the heat-transfer coefficient in the inverted annular flow region. The Bromley-type equation used is

$$Q = 0.943\left[\frac{k_v^3 \rho_v(\rho_l - \rho_v)g\lambda'}{\mu_v(T_w - T_l)L}\right]^{0.25}(T_w - T_l), \qquad [19]$$

where

$$\lambda' = h_{fg}\left[1 + \frac{0.4T\,c_{pv}}{h_{fg}}\right],$$

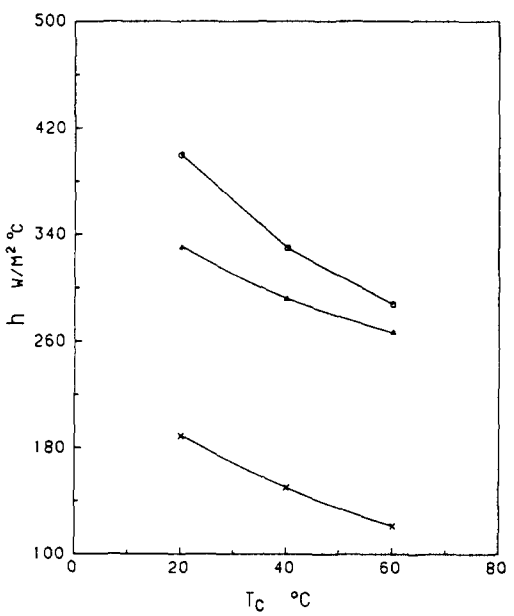

Figure 4. Effect of coolant inlet subcooling on the heat-transfer coefficient. $G = 200\ \text{kg/m}^2\text{s}$, $T_w = 550°\text{C}$. ○, Experimental; ▲, present analysis; ×, Bromley-type equation.

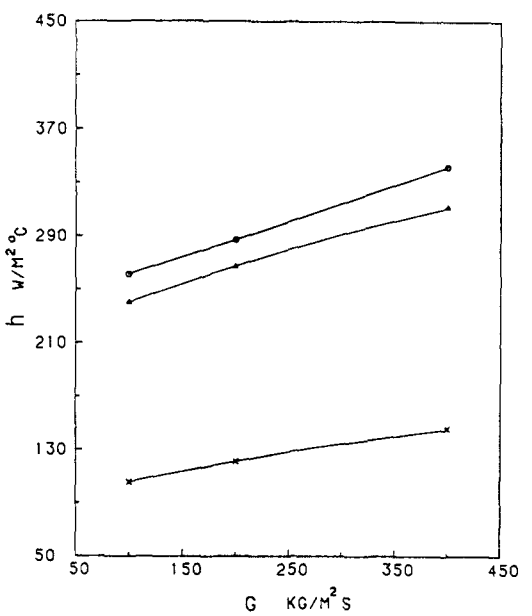

Figure 5. Effect of coolant inlet temperature on the heat-transfer coefficient. $T_w = 550°\text{C}$, $T_c = 60°\text{C}$. ○, Experimental; ▲, present analysis; ×, Bromley-type equation.

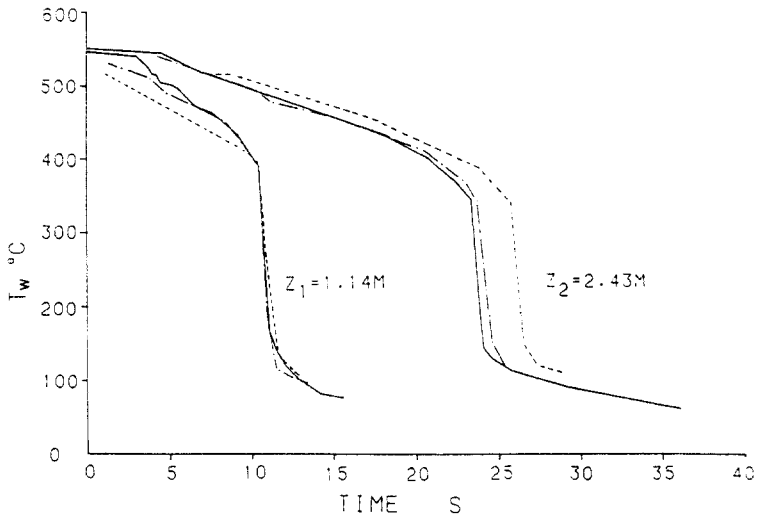

Figure 6. Temperature–time trace curves. $G = 200$ kg/m^2 s, $T_c = 20$°C. ——, Experimental; —·—, present analysis; – – –, Bromley-type equation.

k is the thermal conductivity, h_{fg} is the enthalpy of vaporization and L is the distance from the rewetting front.

In figure 3, we can see that, compared to the Bromley-type heat-transfer coefficient, the heat-transfer coefficient from the present analysis is much closer to the experimental results.

The effects of inlet subcooling and coolant flow rate on the heat-transfer coefficient are shown in figures 4 and 5. It can be seen that both the experimental and analytical results increase with increasing inlet subcooling and coolant flow rate. This agrees qualitatively with the finding of Chan & Yadigaroglu (1980), whose experimental and analytical study also showed increasing heat transfer with increasing coolant flow rate and subcooling.

In general, all other comparisons for different experimental conditions demonstrated that the heat-transfer coefficient obtained by the present analysis is much closer to the experimental coefficient than that obtained by the Bromley-type equation. This indicates that the present method of calculating the heat-transfer coefficient in the inverted annular flow region is a significant improvement over the Bromley-type equation or other pool boiling based equations.

As stated previously, we have shown (Kim & Lee 1982) that the two most important parameters which affect the rewetting velocity are the rewetting temperature and the heat-transfer rate in the

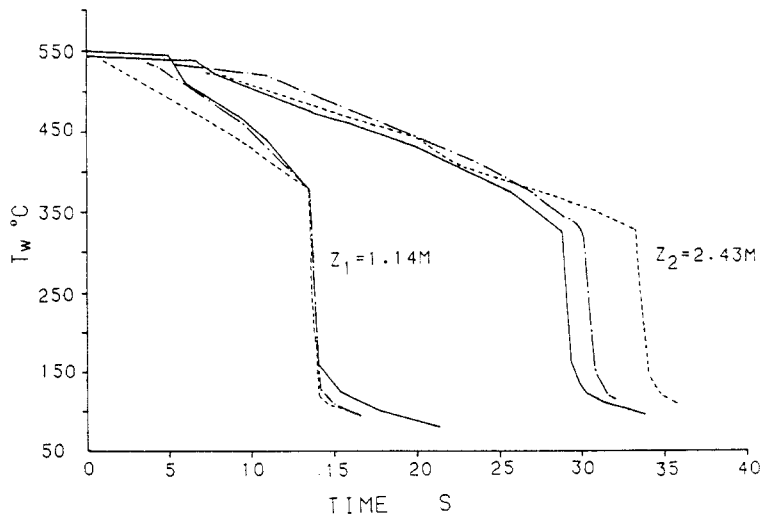

Figure 7. Temperature–time trace curves. $G = 200$ kg/m^2 s, $T_c = 40$°C. ——, Experimental; —·—, present analysis; – – –, Bromley-type equation.

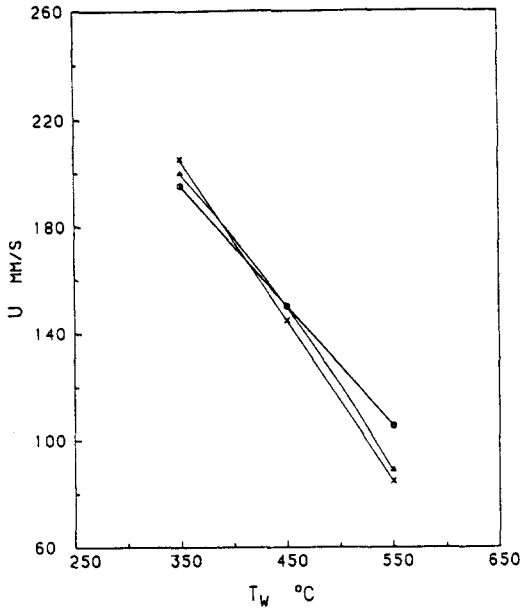

Figure 8. Effect of initial wall temperature on the rewetting velocity. $G = 400\ \text{kg/m}^2\text{s}$, $T_c = 60°\text{C}$. ○, Experimental; ▲, present analysis; ×, Bromley-type equation.

region downstream of the rewetting front. Therefore, the heat-transfer coefficient of the inverted annular flow region obtained in the present analysis was tried in the authors' previous computer simulation model to determine whether it will improve prediction of the rewetting velocity.

The computer simulation predicts the T–T plot at various axial locations of the vertical circular channel under bottom flooding conditions, thus predicting the rewetting rate of a hot vertical channel.

In the simulation, the rewetting process was divided into six heat-transfer regions, namely: single-phase steam, dispersed flow, inverted annular flow, transition boiling, nucleate boiling and single-phase liquid region.

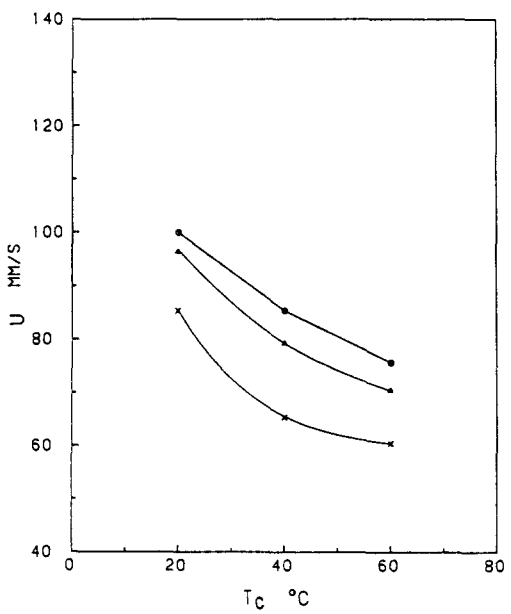

Figure 9. Effect of coolant inlet temperature on the rewetting velocity. $G = 200\ \text{kg/m}^2\text{s}$, $T_w = 550°\text{C}$. ○, Experimental; ▲, present analysis; ×, Bromley-type equation.

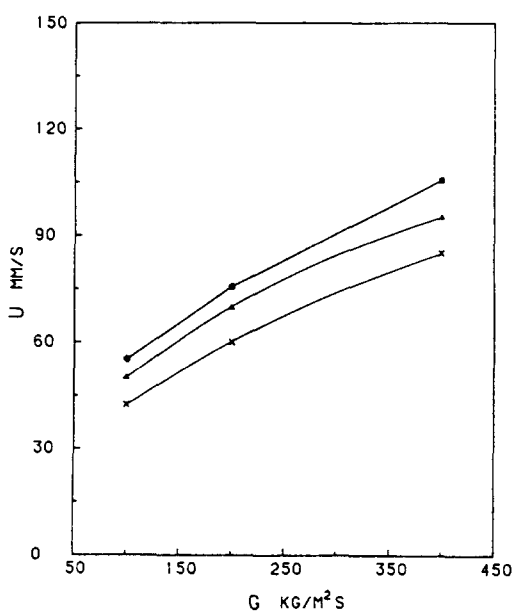

Figure 10. Effect of coolant flow rate on the rewetting velocity. $T_w = 550°\text{C}$, $T_c = 60°\text{C}$. ○, Experimental; ▲, present analysis; ×, Bromley-type equation.

For the rewetting temperature, the empirical equation for bottom flooding by the authors (Kim & Lee 1979), which accurately correlated the rewetting temperature experimentally determined from the in-reactor tests (Gunnerson & Yackle 1981), was used.

Figures 6 and 7 show the comparison of the experimental T–T plots with those predicted with the present analytical results and also those previously calculated using the Bromley-type equation for the inverted annular flow region.

Since the rewetting velocity, U, is obtained from two T–T plots at different locations of the test tube through knowledge of the "rewetting time" and the location of the T–T trace curve, the present analysis should predict the rewetting velocity, U. This is closer to the experimental value than values obtained with the previous analysis. Figures 8–10 show the general pattern of the rewetting velocity over various parameters.

Both the analytical and experimental rewetting velocities, show the same pattern of increasing value with increasing coolant flow rate and inlet subcooling, and with decreasing initial wall temperature. In all three figures, it is seen that the calculated T–T plots using the present analysis are much closer to the experimental T–T plots than the T–T plots calculated using the Bromley-type equation.

The main objective of the present analysis was to obtain a method of calculating accurate heat-transfer coefficients in the inverted annular flow region and to reconfirm the findings of our previous study (Kim & Lee 1982), which states that the two major parameters which affect the rewetting process in a confined space are the heat-transfer rate immediately downstream of the rewetting front, and the rewetting temperature. Both objectives are achieved in the present study.

4. CONCLUSION

The results show that the present analysis gives a heat-transfer coefficient in the inverted annular film boiling region whose value is very close to the experimental one. Also, the results of the analysis reconfirmed that having more accurate heat-transfer coefficients in the immediate downstream of the rewetting front in a confined space improves the computation of rewetting velocities substantially.

Acknowledgement—The financial support for the present study provided by NSERC (Natural Science and Engineering Research Council of Canada, Grant No. A5175) is gratefully acknowledged.

REFERENCES

BARROW, H. 1960 Semi-theoretical solution of asymmetric heat transfer in annular flow. *J. Mech. Engng Sci.* **2,** 331–336.

BROMLEY, L. A. 1950 Heat transfer in stable film boiling. *Chem. Engng Prog.* **46,** 221–227.

CHAN, K. C. & YADIGAROGLU, G. 1980 Calculation of film boiling heat transfer above the quench front during reflooding. Presented at *19th Natn. Heat Transfer Conf.* Orlando, Fla.

CLEMENT, P., DERUAZ, R., RAYMOND, P., REGNIER, P. & REOCREUX, M. 1977 Development of reflood codes FLIRA and PSCHIT: physical modeling and interpretation of ersec experiments. Presented at *5th A. Water Reactor Safety Research Information Mtg*, Washington, D.C.

DEISSLER, R. G. 1955 Turbulent heat transfer and friction in the entrance regions of smooth passages. *Trans. ASME* **88,** 1221–1223.

GROENEVELD, D. G. & GARDINER, S. R. M. 1977 Post-CHF heat transfer under forced convective conditions. Report AECL-5883.

GUNNERSON, F. S. & YACKLE, T. R. 1981 Quenching and rewetting of nuclear fuel rods. *Nucl. Technol.* **51,** 113–117.

KIM, A. K. & LEE, Y. 1979 A correlation of rewetting temperature. *Lett. Heat Mass Transfer* **6,** 117–126.

KIM, A. K. & LEE, Y. 1982 A numerical and experimental study of the rewetting process in bottom flooding. *Proc. 7th Int. Heat Transfer Conf.* **4,** 181–187.

LEE, Y. & PARK, S. D. 1971 Developing turbulent flow in concentric annuli: an analytical study. *Warme-u. Stoffubertrag.* **4,** 156–166.

LEUNG, E. Y., KAYS, W. M. & REYNOLDS, W. C. 1962 Heat transfer with turbulent flow in concentric and eccentric annuli with constant and variable heat flux. Report AHT4, Stanford Univ., Stanford, Calif.

LEVY, S. 1967 Turbulent flow in an annulus. *J. Heat Transfer* **89,** 25–31.

MARTINELLI, R. C. & NELSON, D. B. 1948 Prediction of pressure drop during forced circulation boiling of water. *Trans. ASME* **70,** 695–702.

REICHARDT, H. 1951 Complete representation of turbulent velocity distribution in a smooth pipe. *Z. angew. Math. Mech.* **31,** 208–219.

ROBERTS, A. 1967 A comment on the turbulent flow velocity profile in a concentric annulus. *Int. J. Heat Mass Transfer* **10,** 709–712.